



City Research Online

## City, University of London Institutional Repository

---

**Citation:** Takeishi, K., Kawahara, G., Wakabayashi, H., Uhlmann, M. & Pinelli, A. (2015). Localized turbulence structures in transitional rectangular-duct flow. *Journal of Fluid Mechanics*, 782, pp. 368-379. doi: 10.1017/jfm.2015.546

This is the accepted version of the paper.

This version of the publication may differ from the final published version.

---

**Permanent repository link:** <https://openaccess.city.ac.uk/id/eprint/14266/>

**Link to published version:** <https://doi.org/10.1017/jfm.2015.546>

**Copyright:** City Research Online aims to make research outputs of City, University of London available to a wider audience. Copyright and Moral Rights remain with the author(s) and/or copyright holders. URLs from City Research Online may be freely distributed and linked to.

**Reuse:** Copies of full items can be used for personal research or study, educational, or not-for-profit purposes without prior permission or charge. Provided that the authors, title and full bibliographic details are credited, a hyperlink and/or URL is given for the original metadata page and the content is not changed in any way.

---

---

---

City Research Online:

<http://openaccess.city.ac.uk/>

[publications@city.ac.uk](mailto:publications@city.ac.uk)

---

**Localized turbulence structures in transitional rectangular-duct flow**

Journal:	<i>Journal of Fluid Mechanics</i>
Manuscript ID:	Draft
mss type:	Rapids
Date Submitted by the Author:	n/a
Complete List of Authors:	Takeishi, Keisuke; Osaka University, Department of Mechanical Science Kawahara, Genta; Osaka University, Department of Mechanical Science Uhlmann, Markus; Karlsruhe Institute of Technology, Institute for Hydromechanics Pinelli, Alfredo; City University London, School of Mathematics, Computer Science and Engineering
Keyword:	Transition to turbulence < Instability, Turbulent Flows

# Localized turbulence structures in transitional rectangular-duct flow

KEISUKE TAKEISHI<sup>1</sup>, GENTA KAWAHARA<sup>1,†</sup>,  
HIROKI WAKABAYASHI<sup>1</sup>, MARKUS UHLMANN<sup>2</sup>  
and ALFREDO PINELLI<sup>3</sup>

<sup>1</sup>Graduate School of Engineering Science, Osaka University, Toyonaka 560–8531, Japan

<sup>2</sup>Institute for Hydromechanics, Karlsruhe Institute of Technology, Karlsruhe 76131, Germany

<sup>3</sup>School of Mathematics, Computer Science and Engineering, City University London, London EC1V 0HB, UK

(Received 12 October 2014)

Direct numerical simulations of transitional flow in a rectangular duct of cross-sectional aspect ratio  $A \equiv s/h = 1\text{--}9$  ( $s$  and  $h$  being the duct half span and half height, respectively) have been performed in the Reynolds number range  $Re \equiv u_b h/\nu = 650\text{--}1500$  ( $u_b$  and  $\nu$  being the bulk velocity and the kinematic viscosity, respectively) in order to investigate the dependence on the aspect ratio of spatially localized turbulence structures. It was observed that the marginal Reynolds number  $Re_T$  for sustaining turbulence monotonically decreases from  $Re_T = 730$  for  $A = 1$  (square duct) with increasing aspect ratio and for  $A = 5$  it nearly attains a minimal value  $Re_T \approx 670$  which is consistent with the onset Reynolds number of turbulence in a plane channel ( $A = \infty$ ). Marginally turbulent states consist of localized structures which undergo a fundamental change around  $A = 4$ . At marginal Reynolds numbers turbulence for  $A = 1\text{--}3$  is streamwise-localized similar to turbulent puffs in pipe flow, while for  $A = 5\text{--}9$  turbulence at marginal Reynolds numbers is also localized in the spanwise direction, similar to turbulent spots in plane channel flow. This structural change in marginal states is attributed to the exclusion of turbulence from the vicinity of the duct side-walls in the case of a wide duct with  $A \gtrsim 4$ : here the wall shear rate on the side-walls is so low (and thus friction length is so long) that a self-sustaining minimal flow unit of streamwise vortices and streaks is larger than the duct height and, therefore, it cannot be accommodated.

**Key words:** Transition to turbulence, Turbulent flows

---

## 1. Introduction

Subcritical transition to turbulence can be triggered only by finite-amplitude perturbations. Since a fully nonlinear description is therefore indispensable for the transition, the elucidation of transition mechanisms and structures is much more challenging than in the case of supercritical transition. Subcritical turbulence transition in wall-bounded shear flows is known to be characterized in terms of the emergence of well-organized turbulence patches bounded by laminar regions. In circular pipe flow streamwise-localized turbulence has been observed by many investigators (see Mullin 2011). It is widely accepted that there are two kinds of localized turbulence structures, a puff and a slug (Wyganski & Champagne 1973). Turbulent puffs appear at lower Reynolds number than slugs to

† Email address for correspondence: kawahara@me.es.osaka-u.ac.jp

2 *K. Takeishi, G. Kawahara, H. Wakabayashi, M. Uhlmann and A. Pinelli*

play a role in the early stage of transition. At low Reynolds numbers puffs can be in an equilibrium state where they have roughly 20 pipe diameter length (Mullin 2011) and propagate at a speed of approximately 0.9 times the bulk mean velocity (Nishi *et al.* 2008; Wygnanski & Champagne 1973). The lowest value of the onset Reynolds number (based on the pipe diameter and the bulk mean velocity) of equilibrium puffs was estimated to be 1750 by Peixinho & Mullin (2006). In plane channel flow, on the other hand, two types of localized structures have been observed: one is a turbulent spot localized not only in the streamwise direction but also in the spanwise direction (Carlson *et al.* 1982), and the other is a turbulent stripe localized in the direction inclined from the streamwise direction in the spanwise direction (Hashimoto *et al.* 2009). Turbulent spots first arise at lower Reynolds numbers, and as the Reynolds number increases they develop into stripes through their growth and subsequent break-up (Aida *et al.* 2010). Spots grow spatially in time, and their leading (or trailing) edge propagates at a speed of about 1.0–1.3 (or 0.5–0.8) bulk velocity (Carlson *et al.* 1982; Lemoult *et al.* 2013). An equilibrium state of spots like that of puffs has not been reported even at their onset, and equilibrium structures in a plane channel might be turbulent stripes rather than spots (Aida *et al.* 2010). The onset Reynolds number (based on channel height and bulk velocity) of spots is around 1333 (Carlson *et al.* 1982; Hashimoto *et al.* 2009).

The characteristics of subcritical transition to turbulence in rectangular-duct flow, including the shape of localized structures, should depend on cross-sectional aspect ratio  $A$  of the duct, where  $A = s/h$  ( $\geq 1$ ),  $s$  ( $\geq h$ ) and  $h$  being the duct half span and half height, respectively. In the case of a square duct ( $A = 1$ ), on one hand, the transition characteristics are believed to be similar to those of pipe flow, and the appearance of streamwise-localized structures can be expected in a marginally turbulent state similar to turbulent puffs in a pipe. In the limit of  $A \rightarrow \infty$ , on the other hand, the rectangular duct becomes equivalent to a plane channel such that the transition to turbulence will resemble that of plane channel flow, and marginal turbulence is represented by streamwise- and spanwise-localized structures, i.e. turbulent spots. Now the question arises: What is the structure of localized turbulence in transitional rectangular-duct flow for finite values of  $A$  larger than unity? In the present study, in order to reply to this question, direct numerical simulations of rectangular-duct flow were performed at transitional Reynolds numbers using a pseudospectral method (Pinelli *et al.* 2010; Uhlmann *et al.* 2007) in a long computational domain. It is shown how the marginal Reynolds number for sustained turbulence and the structure of marginally turbulent states depend on the geometrical aspect ratio of the duct. The dependence of marginal turbulence structures is interpreted in the light of scaling arguments with local wall units. Finally, the structural change of localized turbulence when increasing the Reynolds number is analyzed.

## 2. Flow configuration and numerical simulations

We consider the motion of an incompressible viscous fluid through an infinitely long duct with a rectangular cross-section of half height  $h$  and half span  $s$  ( $\geq h$ ). The fluid motion is driven by a constant flow rate  $F$ , and the bulk mean velocity  $u_b = F/(4sh)$  is temporally invariant. A right-handed Cartesian coordinate system  $(x, y, z)$  is introduced with its origin on the centre axis along which the coordinate  $x$  is defined. The coordinates  $y$  and  $z$  are taken in the height direction and the spanwise direction, respectively. The velocity components are denoted by  $u$ ,  $v$  and  $w$  along the  $x$ -,  $y$ - and  $z$ -directions, respectively. No-slip and impermeable conditions  $u = v = w = 0$  are imposed on the duct walls, and the flow field is assumed to be periodic of length  $L_x$  in the  $x$ -direction. The

---

$A$	$Re_T$	$Re_\tau$	$\Delta x u_\tau / \nu$	$\max(\Delta y u_\tau / \nu)$	$\max(\Delta z u_\tau / \nu)$
1	730	52.5	6.45	2.58	2.58
2	710	48.8	5.99	2.40	2.40
3	690	47.3	5.82	2.33	2.33
4	685	45.7	5.61	2.24	2.24
5	675	45.6	5.60	2.24	2.21
9	670	46.6	5.72	2.29	2.57

---

TABLE 1. Simulation parameters in typical runs

dimensionless control parameters are the Reynolds number  $Re = u_b h / \nu$  and the aspect ratio  $A = s/h$  ( $\geq 1$ ), where  $\nu$  is the kinematic viscosity of the fluid.

We solve numerically the incompressible Navier–Stokes equations with a fractional-step method (see Pinelli *et al.* 2010, for the details of the numerical method and its validation). The time integration is based on the Crank–Nicolson scheme for the viscous terms and a three-step Runge–Kutta method for the nonlinear terms including the pressure term. The flow variables are expanded in terms of truncated Fourier series in the  $x$ -direction and Chebyshev polynomials in the  $(y, z)$ -directions. We use a collocated grid arrangement in physical space constructed from an equidistant spacing  $\Delta x$  in the  $x$ -direction and the Chebyshev–Gauss–Lobatto points in the  $(y, z)$ -directions. The nonlinear terms are evaluated in physical space whereas the explicit contribution of the linear terms is evaluated in spectral space. The fields are transformed back and forth by means of fast Fourier transform and fast cosine transform. De-aliasing according to the 2/3-rule is performed in the  $x$ -direction. In numerical simulations the aspect ratio is set at  $A = 1, 2, 3, 4, 5, 9$  and the Reynolds number  $Re$  is changed in the range of  $650 \leq Re \leq 1500$ . In all the simulations the streamwise period is fixed at  $L_x = 40\pi h$ .

### 3. Identifications of marginal turbulence

We first identify the marginal Reynolds numbers  $Re_T$  which allow sustaining turbulence for  $A = 1$ –9. For each value of  $A$  the Reynolds number  $Re$  of the flow is gradually reduced by 5 units from  $Re = 1500$  at which a fully developed turbulent state can be observed. After each reduction of  $Re$  the computations are run until either the flow re-laminarizes or a minimum time  $900u_\tau^2/\nu$  has elapsed, where  $u_\tau = \sqrt{\tau/\rho}$  is the friction velocity,  $\tau$  and  $\rho$  being the averaged wall shear stress over the four walls and time, and the mass density of the fluid, respectively. The sustenance of turbulence is verified at every time step by monitoring the maximum value of the (positive) second invariant  $Q$  of the velocity gradient tensor (which represents vortex structures) over the whole flow field. If the maximum value of  $Q(\nu/u_\tau^2)^2$  is greater than  $2 \times 10^{-3}$ , then the turbulence is judged to survive at that time. For each value of the aspect ratio simulations are run with five distinct initial data among which the lowest value is identified as the marginal Reynolds number henceforth denoted as  $Re_T$ . It has been checked that changes in the threshold value for  $Q(\nu/u_\tau^2)^2$  do not lead to significant difference in  $Re_T$ . The simulation parameters in the typical runs where the marginal Reynolds numbers have been identified are shown in table 1. Therein  $Re_\tau = u_\tau h / \nu$  denotes the friction Reynolds number, and  $\Delta y$  and  $\Delta z$  are the grid intervals in the  $y$ - and  $z$ -directions, respectively.

In the present identification a relatively short duration time  $900u_\tau^2/\nu$  has been taken, because localized marginal turbulence will always decay after its finite lifetime whose probability distribution is exponential (Hof *et al.* 2006), in other words localized turbu-

4 *K. Takeishi, G. Kawahara, H. Wakabayashi, M. Uhlmann and A. Pinelli*

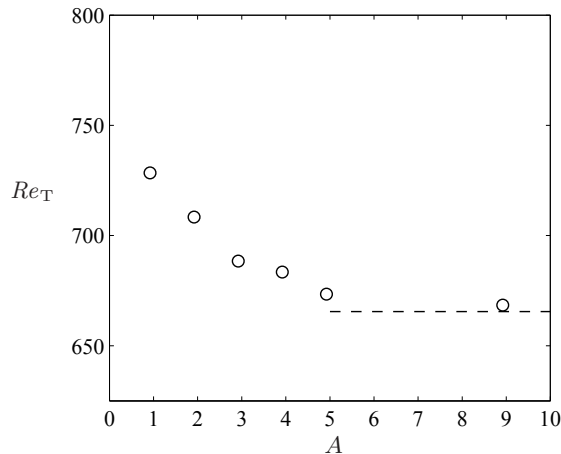


FIGURE 1. The marginal Reynolds number  $Re_T$  as a function of the aspect ratio  $A$ . The dashed horizontal line denotes the value of  $Re_T = 667$ .

lence is transient. If the duration time were longer, therefore, much higher values for  $Re_T$  would be obtained. Near-wall turbulence is known to survive by the regeneration cycle consisting of streamwise vortices and streaks (Hamilton *et al.* 1995), and the period of the cycle is about  $282u_\tau^2/\nu$  at the Reynolds number  $Re = 1333$  in the minimal flow unit ( $\pi h \times 2h \times 0.35\pi h$ ) of plane channel turbulence (Jiménez & Moin 1991). In this study, accordingly, the duration time has been set to be short in bulk time units but longer than the period of the near-wall regeneration cycle. A change of the duration time to  $900u_\tau^2/\nu - 400u_\tau^2/\nu$  (or  $+400u_\tau^2/\nu$ ) was found to lead only to a slight variation of the marginal Reynolds number by  $-2.5$  (or  $+10.8$ ) on average.

Figure 1 shows the dependence of the marginal Reynolds number  $Re_T$  on the aspect ratio  $A$ . The marginal Reynolds number for a square duct measures  $Re_T = 730$  which is lower than the recently reported critical Reynolds number,  $Re \approx 1100$ , in a square duct with minimal streamwise extension (Uhlmann *et al.* 2007). It is also lower than the onset Reynolds number (based on a pipe radius),  $Re = 875$ , of turbulent puffs in pipe flow (Peixinho & Mullin 2006). Let us define an equivalent radius of a square duct with half height  $h$  in the sense of a consistent cross-sectional area as  $r = (2/\sqrt{\pi})h$ ; the marginal Reynolds number corresponding to pipe flow can then be expressed as  $(r/h)Re_T = 824$  which is much closer to the reported value 875. It can be seen from figure 1 that the marginal Reynolds number decreases monotonically with increasing  $A$ . When based on the maximum velocity of a laminar profile for a fixed bulk velocity the reduction of the marginal Reynolds number (not shown) is even more striking than that of  $Re_T$  shown in figure 1. The monotonic decrease of  $Re_T$  is thought intuitively to be a consequence of the weaker constraint which the side-walls in the wider duct impose on the flow. The stabilization of infinitesimal disturbances by the side-walls has also been found in laminar rectangular-duct flow (Tatsumi & Yoshimura 1990). For  $A = 5$ , however, the marginal Reynolds number nearly attains the minimal value of  $Re_T \approx 670$  which is comparable to the onset Reynolds number for sustaining turbulent spots in a plane channel (Carlson *et al.* 1982; Hashimoto *et al.* 2009).

#### 4. Structures of marginal turbulence

We next discuss the turbulence structures at the marginal Reynolds numbers  $Re = Re_T$  for each geometrical aspect ratio. In figure 2 are shown marginal vortex structures visu-

## Localized turbulence in rectangular-duct flow

5

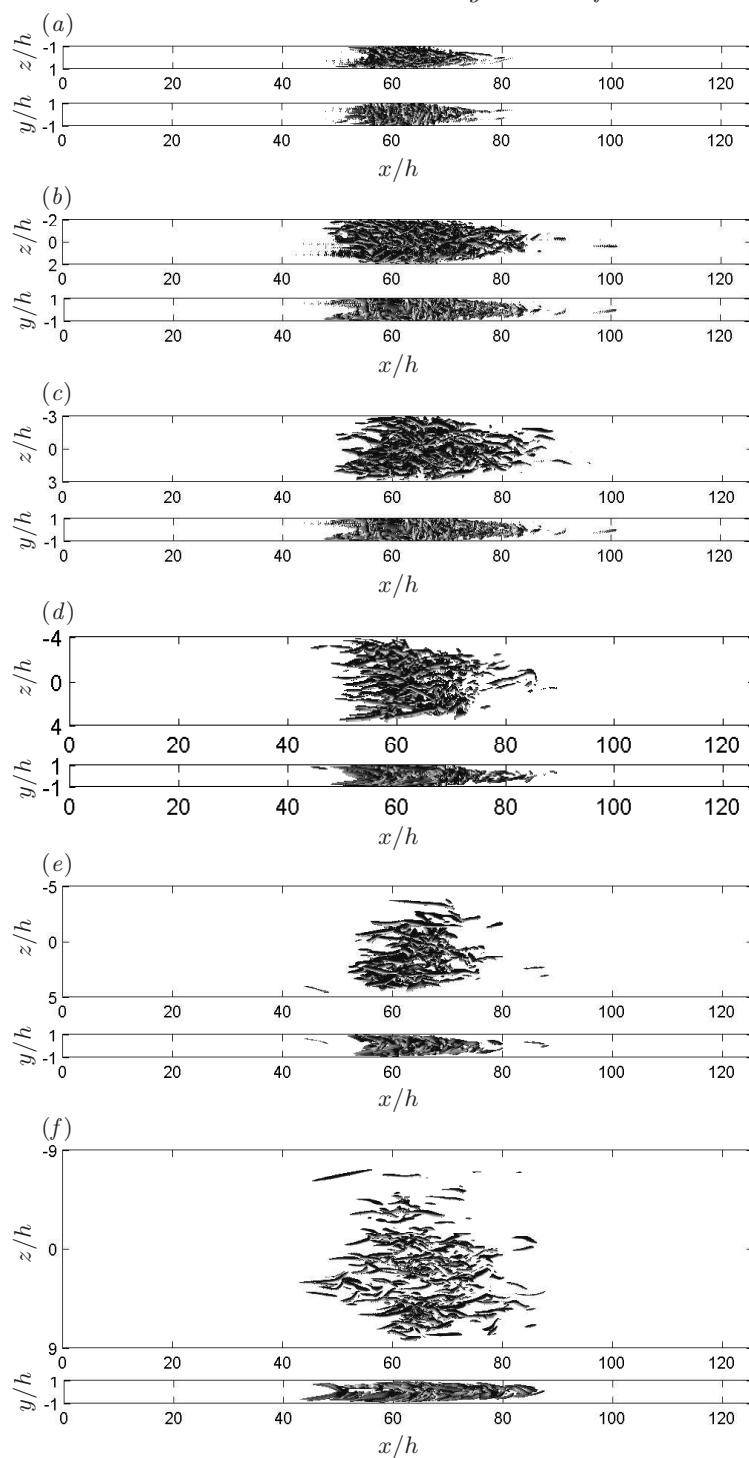


FIGURE 2. Instantaneous vortical structures visualized by isosurfaces of the second invariant of the velocity gradient tensor,  $Q (\nu/u_\tau^2)^2 = 2 \times 10^{-3}$  at the marginal Reynolds numbers  $Re = Re_T$  (see table 1 for the values of  $Re_T$  for each  $A$ ). (a)  $A = 1$ , (b)  $A = 2$ , (c)  $A = 3$ , (d)  $A = 4$ , (e)  $A = 5$ , (f)  $A = 9$ . All the localized structures have been centered in the  $x$ -direction.

6 *K. Takeishi, G. Kawahara, H. Wakabayashi, M. Uhlmann and A. Pinelli*

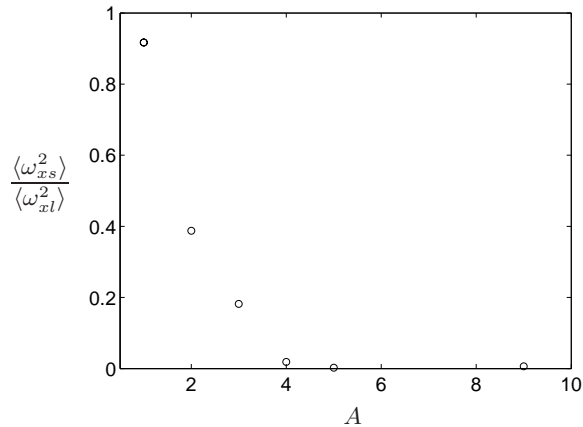


FIGURE 3. The relative turbulence intensity  $\langle \omega_{xs}^2 \rangle / \langle \omega_{xl}^2 \rangle$  on the side-walls as a function of  $A$ .

alized by positive isosurfaces of the second invariant of the velocity gradient tensor. It is observed that marginal turbulence structures exhibit spatial localization for all the values of  $A$ . Localized turbulence can be seen to be composed of a large number of streamwise tubular vortices. For aspect ratios close to unity ( $A = 1-3$ ) there appear streamwise-localized clusters of vortical structures which are strikingly similar to turbulent puffs in pipe flow (Wynanski & Champagne 1973). Similar to equilibrium puffs in pipe flow the localized clusters for  $A = 1-3$  do not extend or shrink in time, and their streamwise extent is about  $30h-40h$  which is comparable with approximate 20 diameter length of the equilibrium puffs (Mullin 2011). For the larger aspect ratio ( $A = 4, 5, 9$ ), on the other hand, the vortical structures are found to disappear from the vicinity of the side-walls ( $A = 4$ ), and the vortical clusters are localized not only in the streamwise direction but also in the spanwise direction ( $A = 5, 9$ ). The roundish clusters for  $A = 5, 9$  in figure 2 are reminiscent of turbulent spots in plane channel flow.

In the wider duct a spanwise localization of turbulence has been found in figure 2; however, this result might be subject to the choice of the threshold of isosurfaces. In order to supplement the demonstration of this crucial structural change with  $A$ , we shall compare turbulence intensity on the side-walls  $z/h = \pm A$  with that of the longer two walls  $y/h = \pm 1$ . As typical turbulence intensity on the walls, let us take the average,  $\langle \omega_{xs}^2 \rangle$  or  $\langle \omega_{xl}^2 \rangle$ , of the squared streamwise vorticity on the side-walls or the longer walls. Here the average is performed over time and over the “vigorous streamwise extent”, the latter being defined as the streamwise interval in which  $\langle \omega_x^2 \rangle_{yz} \geq \frac{1}{2} \max(\langle \omega_x^2 \rangle_{yz})$ ,  $\langle \cdot \rangle_{yz}$  denoting integration over the cross-plane. The turbulence intensity on the side-walls compared with that on the other walls,  $\langle \omega_{xs}^2 \rangle / \langle \omega_{xl}^2 \rangle$ , is shown as a function of  $A$  in figure 3. It can be seen that the relative turbulence intensity on the side-walls attenuates with increasing  $A$ . It is confirmed quantitatively that the turbulence on the side-walls significantly decays for  $A = 4, 5, 9$ . In the ducts of  $A = 5, 9$ , for which turbulent spots have been observed, the turbulence on the side-walls has disappeared almost completely.

The expulsion of turbulence from the vicinity of the side-walls should be a consequence of relaminarization of turbulent flow over the side-walls rather than the other two walls. In order to inspect this aspect we consider the behaviour of the main contributor to near-wall turbulence energy production,  $P = -\langle u'w' \rangle \partial \langle u \rangle / \partial z|_{y/h=0}$ , over the side-wall  $z/h = -A$  along the side-wall bisector, where the average has been taken over time

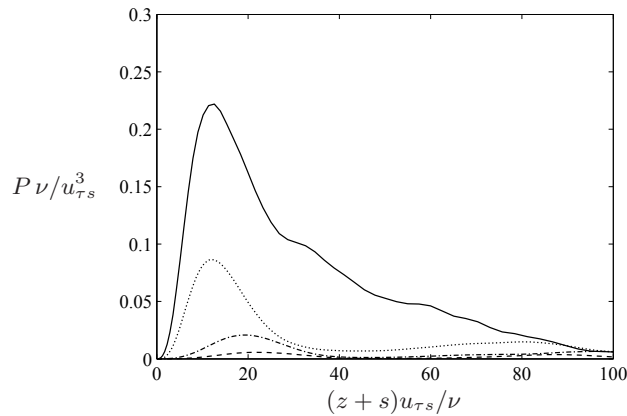


FIGURE 4. The turbulence production  $P$  on the side-wall bisector  $y/h = 0$  as a function of the distance from the side-wall. —,  $A = 2$ ; ·····,  $A = 3$ ; - · - ·,  $A = 4$ ; ----,  $A = 5$ .

and the vigorous streamwise extent, and the prime denotes a fluctuation around the average. As shown in figure 4, the turbulence production for  $A = 2$  possesses a remarkable peak of about  $0.22\nu/u_{\tau_s}^3$  around  $(z+s)u_{\tau_s}/\nu = 12$ , which corresponds to that in a plane channel, where  $u_{\tau_s}$  is the friction velocity averaged on the side-wall over time and the vigorous streamwise extent. This outstanding production stems from buffer-layer streamwise vortices associated with streamwise streaks on the side-wall as in a plane channel. The turbulence production, however, decreases with increasing  $A$ , and for  $A \gtrsim 4$  there is no longer any significant production.

In their numerical simulations of plane channel turbulence Jiménez & Moin (1991) minimized the size of the periodic computational domain while sustaining turbulence activity, obtaining a minimal flow unit with a width of approximately 100 friction lengths, which accommodates a pair of counter-rotating staggered streamwise vortices and one low-velocity streak. If the width of the flow is less than this minimal value, turbulence dies out. Figure 5 shows the full width of the duct along the side-wall normalized with the friction length  $\nu/u_{\tau_s}$  as a function of  $A$ . It can be seen that the normalized width diminishes with increasing  $A$ , measuring approximately 100 for  $A = 2$ –3. This is a direct consequence of the lower wall shear rate (i.e. the increased friction length) on the side-walls of larger-aspect-ratio ducts for the fixed bulk velocity. For  $A \gtrsim 4$  the duct width  $2h$  is smaller than 100 wall units, i.e. it cannot accommodate a minimal flow unit of near-wall turbulence. This is the reason why the flow in the vicinity of the side-walls relaminarizes, so that the spanwise-localized spots arise for  $A \gtrsim 4$ .

## 5. Localized turbulence structures at higher Reynolds number

In the following we briefly discuss the modifications to the localized turbulence when the Reynolds number is increased. Instantaneous vortical structures at  $Re = 800$  (well above  $Re_T$ ) are shown in figure 6. An essential difference from the marginal puff cannot be seen in the duct with aspect ratio close to unity ( $A = 2$ ); however, the turbulent puff in the wider duct ( $A = 3$ ) is skewed in the spanwise direction. The meandering turbulence structures in the much wider duct for  $A = 9$  are remarkably reminiscent of turbulent stripes found in plane channel flow by Hashimoto *et al.* (2009) who observed that the stripes appear in the Reynolds number range  $Re = 850$ –1000. The oblique bands in figure 6(c) could arise from growing spots at the higher Reynolds number, as reported in Aida *et al.* (2010).

8 *K. Takeishi, G. Kawahara, H. Wakabayashi, M. Uhlmann and A. Pinelli*

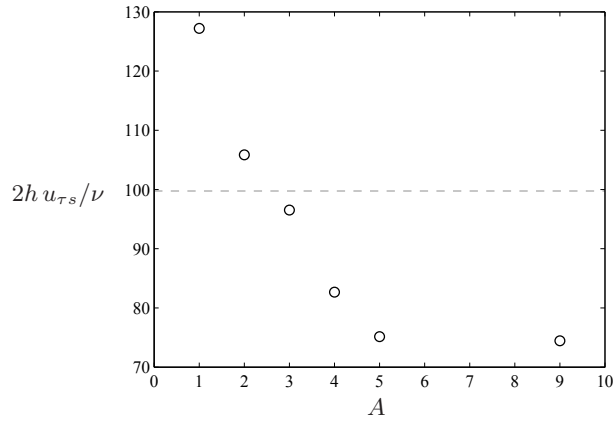


FIGURE 5. The full duct width  $2h$  along the side-wall normalized with the friction length on the side-wall as a function of  $A$ . The dashed horizontal line corresponds to the size  $100\nu/u_{\tau s}$  of a minimal flow unit in plane channel flow.

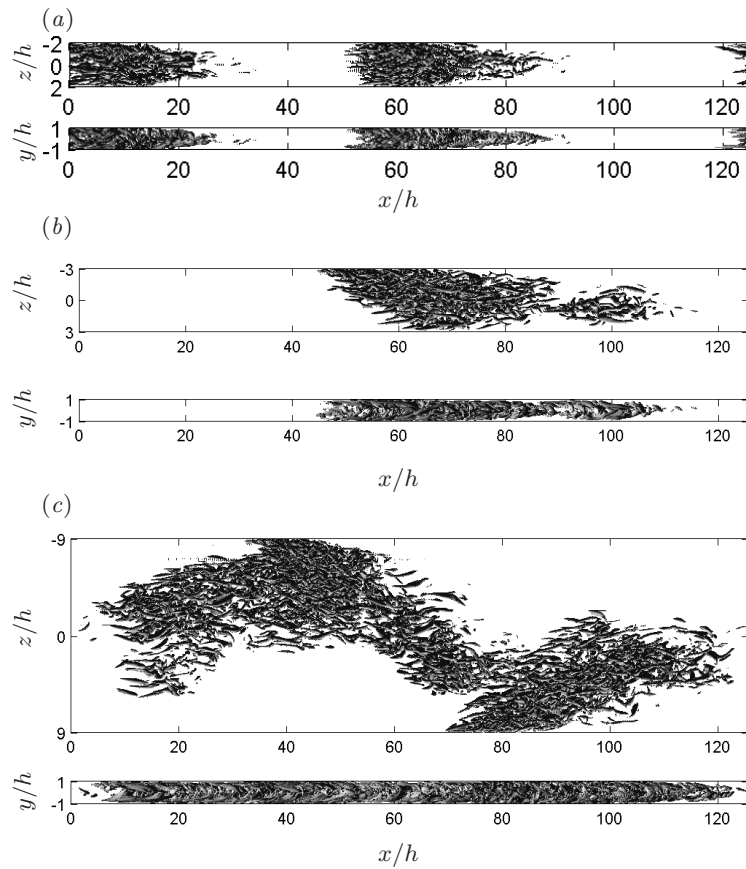


FIGURE 6. Same as figure 2 but for the higher Reynolds number  $Re = 800$  than  $Re_T$ .  
(a)  $A = 2$ , (b)  $A = 3$ , (c)  $A = 9$ .

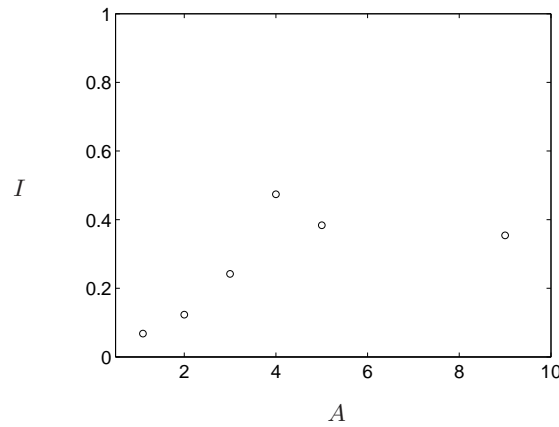


FIGURE 7. The skewness indicator  $I$  of turbulence structures as a function of  $A$  at  $Re = 800$ .

In order to examine quantitatively the dependence on the aspect ratio of the skewness of the localized turbulence at the higher Reynolds number, a skewness indicator is introduced as follows. At a given time  $t$  let us define  $f(x, z, t) = \langle \omega_x^2 \rangle_y / \langle \langle \omega_x^2 \rangle_y \rangle_{xz}$  as a two-dimensional ‘distribution function’ of a vortical cluster, where  $\langle \cdot \rangle_{xz}$  denotes the  $(x, z)$ -integration in the vigorous streamwise extent and  $\langle \cdot \rangle_y$  integrating over the  $y$ -direction. The relative coordinates  $(x', z')$  with respect to the centre of the vortical cluster are then defined as  $x' = x - \langle xf \rangle_{xz}$  and  $z' = z - \langle zf \rangle_{xz}$ . Now we compute the averaged modulus of the ‘cross correlation’ of  $(x', z')$  given by  $I \equiv \overline{\left| \langle x' z' f \rangle_{x' z'} / \sqrt{\langle x'^2 f \rangle_{x' z'} \langle z'^2 f \rangle_{x' z'}} \right|}$  which defines the skewness indicator  $I$ , where  $\overline{(\cdot)}$  represents an ensemble average over 25–70 realizations for each value of  $A$ . In the computations the vigorous streamwise extent of a meandering cluster as in figure 6(c) is split into individual pieces with distinct skewness indicators. As shown in figure 7 the computed skewness of localized turbulence patches gradually increases with increasing  $A$  (except for a kink at  $A = 4$  which is presumably due to a statistical error), attaining a plateau for  $A \gtrsim 4$ .

## 6. Concluding remarks

Direct numerical simulations have been performed for transitional flow in rectangular ducts with various aspect ratios  $A$ . The marginal Reynolds number  $Re_T$  for sustaining turbulence decreases monotonically from  $Re_T = 730$  for a square duct with increasing  $A$  due to the weakening constraint by the side-walls in the wider duct, and for  $A = 5$  it approaches the minimal value  $Re_T \approx 670$  comparable to the onset Reynolds number of plane channel turbulence. Marginally turbulent states are characterized by spatially localized structures: there appear streamwise-localized turbulent puffs for  $A = 1$ –3, while streamwise- and spanwise-localized turbulent spots emerge for  $A = 5$ –9. Puff-spot transition in localized marginal turbulence has been found for  $A \approx 4$ . The disappearance of turbulence from the vicinity of the side-walls is responsible for this critical change of the localized structures. In the wider duct flow with  $A \gtrsim 4$  the wall shear rate is so low (and thus the friction length is so long) on the side-walls that a self-sustaining minimal flow unit of streamwise vortices and low-velocity streaks is larger than the duct height and, therefore, it cannot be accommodated.

The phenomenological interpretation of the spanwise localization of marginal turbulence leading to turbulent spots for rectangular-duct flow, proposed in this paper should

10 *K. Takeishi, G. Kawahara, H. Wakabayashi, M. Uhlmann and A. Pinelli*

be followed by a theoretical demonstration. One candidate for a theoretical approach would be the characterization of localized structures in terms of invariant solutions to the Navier–Stokes equation (see Kawahara *et al.* 2012). Recently, a streamwise-localized relative periodic solution has been discovered in pipe flow (Avila *et al.* 2013) while a streamwise- and spanwise-localized relative periodic solution has been found in plane channel flow (Zammert & Eckhardt 2014). In rectangular-duct flow, to our knowledge, there are no reports of spatially localized invariant solutions; however, our own preliminary study suggests that a travelling-wave solution for  $A = 1$  recently obtained by Uhlmann *et al.* (2010) would exhibit the spanwise localization when tracked to  $A > 1$ . This latest finding might be a good starting point for a future theoretical demonstration of turbulence localization in transitional rectangular-duct flow.

This work was partially supported by a Grant-in-Aid for Scientific Research (Grant Numbers 25249014, 26630055) from the Japanese Society for the Promotion of Science.

#### REFERENCES

- AIDA, H., TSUKAHARA, T. & KAWAGUCHI, Y. 2010 DNS of turbulent spot developing into turbulent stripe in plane Poiseuille flow. In *Proceedings of ASME 2010 3rd Joint US-European Fluids Engineering Summer Meeting*, pp. 2125–2130.
- AVILA, M., MELLBOVSKY, F., ROLAND, N. & HOF, B. 2013 Streamwise-localized solutions at the onset of turbulence in pipe flow. *Phys. Rev. Lett.* **110**, 224502.
- CARLSON, D., WIDNALL, S. & PEETERS, M. 1982 Flow-visualization study of transition in plane Poiseuille flow. *J. Fluid Mech.* **121**, 487–505.
- HAMILTON, J. M., KIM, J. & WALEFFE, F. 1995 Regeneration mechanisms of near-wall turbulence structures. *J. Fluid Mech.* **287**, 317–348.
- HASHIMOTO, S., HASOBE, A., TSUKAHARA, T., KAWAGUCHI, Y. & KAWAMURA, H. 2009 An experimental study on turbulent-stripe structure in transitional channel flow. In *Proceedings of the Sixth International Symposium on Turbulence, Heat and Mass Transfer*, pp. 193–196.
- HOF, B., WESTERWEEL, J., SCHNEIDER, T. M. & ECKHARDT, B. 2006 Finite lifetime of turbulence in shear flows. *Nature* **443**, 59–62.
- JIMÉNEZ, J. & MOIN, P. 1991 The minimal flow unit in near-wall turbulence. *J. Fluid Mech.* **225**, 213–240.
- KAWAHARA, G., UHLMANN, M. & VAN VEEN, L. 2012 The significance of simple invariant solutions in turbulent flows. *Ann. Rev. Fluid Mech.* **44**, 203–225.
- LEMOULT, G., J.-L.AIDER & WESFREID, J. E. 2013 Turbulent spots in a channel: large-scale flow and self-sustainability. *J. Fluid Mech.* **731**, R1.
- MULLIN, T. 2011 Experimental studies of transition to turbulence in a pipe. *Ann. Rev. Fluid Mech.* **43**, 1–24.
- NISHI, M., ÜNSAL, B., DURST, F. & BISWAS, G. 2008 Laminar-to-turbulent transition of pipe flows through puffs and slugs. *J. Fluid Mech.* **614**, 425–446.
- PEIXINHO, J. & MULLIN, T. 2006 Decay of turbulence in pipe flow. *Phys. Rev. Lett.* **96**, 094501.
- PINELLI, A., UHLMANN, M., SEKIMOTO, A. & KAWAHARA, G. 2010 Reynolds number dependence of mean flow structure in square duct turbulence. *J. Fluid Mech.* **644**, 107–122.
- TATSUMI, T. & YOSHIMURA, T. 1990 Stability of the laminar flow in a rectangular duct. *J. Fluid Mech.* **212**, 437–449.
- UHLMANN, M., KAWAHARA, G. & PINELLI, A. 2010 Traveling-waves consistent with turbulence-driven secondary flow in a square duct. *Phys. Fluids* **22**, 084102.
- UHLMANN, M., PINELLI, A., KAWAHARA, G. & SEKIMOTO, A. 2007 Marginally turbulent flow in a square duct. *J. Fluid Mech.* **588**, 153–162.
- WYGNANSKI, I. J. & CHAMPAGNE, F. H. 1973 On transition in a pipe. part 1. the origin of puffs and slugs and the flow in a turbulent slug. *J. Fluid Mech.* **59**, 281–335.
- ZAMMERT, S. & ECKHARDT, B. 2014 Streamwise and doubly-localised periodic orbits in plane Poiseuille flow. Preprint, <http://arxiv.org/abs/1404.2582v2>.